

Role of Peptidoglycan Amidases in the Development and Morphology of the Division Septum in *Escherichia coli*^{∇†}

Richa Priyadarshini,^{1‡} Miguel A. de Pedro,² and Kevin D. Young^{1*}

Department of Microbiology and Immunology, University of North Dakota School of Medicine, Grand Forks, North Dakota, 58202-9037,¹ and Centro de Biología Molecular Severo Ochoa Consejo Superior de Investigaciones Científicas-Universidad Autónoma de Madrid, Facultad de Ciencias, Madrid, Spain²

Received 21 March 2007/Accepted 23 April 2007

***Escherichia coli* contains multiple peptidoglycan-specific hydrolases, but their physiological purposes are poorly understood. Several mutants lacking combinations of hydrolases grow as chains of unseparated cells, indicating that these enzymes help cleave the septum to separate daughter cells after cell division. Here, we confirm previous observations that in the absence of two or more amidases, thickened and dark bands, which we term septal peptidoglycan (SP) rings, appear at division sites in isolated sacculi. The formation of SP rings depends on active cell division, and they apparently represent a cell division structure that accumulates because septal synthesis and hydrolysis are uncoupled. Even though septal constriction was incomplete, SP rings exhibited two properties of mature cell poles: they behaved as though composed of inert peptidoglycan, and they attracted the IcsA protein. Despite not being separated by a completed peptidoglycan wall, adjacent cells in these chains were often compartmentalized by the inner membrane, indicating that cytokinesis could occur in the absence of invagination of the entire cell envelope. Finally, deletion of penicillin-binding protein 5 from amidase mutants exacerbated the formation of twisted chains, producing numerous cells having septa with abnormal placements and geometries. The results suggest that the amidases are necessary for continued peptidoglycan synthesis during cell division, that their activities help create a septum having the appropriate geometry, and that they may contribute to the development of inert peptidoglycan.**

Most eubacteria produce multiple hydrolases that cleave different bonds within the peptidoglycan (PG or murein) cell wall: amidases remove peptide side chains from the carbohydrate polymer, endopeptidases cleave cross-linked peptides that connect the glycan chains, and lytic transglycosylases hydrolyze the glycan backbone (24, 47). These PG-specific hydrolases were once thought to be essential for inserting new material into the wall during bacterial growth (24, 25), a view based on the reasonable hypothesis that cross-links between the glycan chains had to be broken so that new PG strands could be incorporated into the existing wall (31). However, bacterial growth continues perfectly well in the absence of these dedicated hydrolases, including almost all of the amidases, endopeptidases, and lytic transglycosylases (14, 22, 23), meaning that any bond-breaking during normal cell wall elongation must be performed by other enzymes. So why, then, does *Escherichia coli* carry so many murein-specific hydrolases?

In the gram-positive bacteria, PG hydrolases split the septum that separates daughter cells at the end of cell division. For example, in *Streptococcus pneumoniae*, LytA (an amidase) and LytB (a glucosaminidase) localize to the equatorial and polar regions, respectively, and mutants lacking either hydro-

lase grow in long chains, with double mutants being especially deficient in cell separation (13, 46). In *Bacillus subtilis*, the DL-endopeptidases LytE (CwlF) and LytF (CwlE) accumulate at sites of cell separation, and a *lytE lytF* double mutant forms extraordinarily long chains of cells (38, 55). Because LytE localization requires FtsZ and penicillin-binding protein 2B (PBP2B), this enzyme acts as though it is a hydrolytic component of the division apparatus (9). With these precedents, it is not farfetched to predict that homologous hydrolases perform similar functions in the gram-negative bacteria.

In line with this expectation, deleting multiple hydrolases from *E. coli* produces mutants with cell separation defects (22, 23). For example, *E. coli* mutants lacking the AmiABC amidases grow in long chains of connected cells (22, 23), and AmiC physically localizes to the septal ring during division (4), indicating that these enzymes help separate daughter cells during division. Deleting additional endopeptidase- or transglycosylase-encoding genes enhances the frequency and extent of these separation defects, resulting in an increase in the numbers of cells in chains as well as the length of each chain (22, 23). Another periplasmic murein hydrolase, EnvC, also localizes to the septal ring during cell division (5). Although the specific enzymatic activity of EnvC is unknown, an *envC* mutant has a normal amount of amidase (30), one protein domain resembles a zinc metallopeptidase, and EnvC (YipA) hydrolyzes β -casein (28), all of which are consistent with the activity of an endopeptidase rather than an amidase or glycosylase. EnvC apparently localizes to the nascent division site prior to the start of active invagination because 38% of EnvC-rings are not associated with visible constrictions (5). Consistent with this supposition is the fact that *envC* mutants have much shallower constrictions than those observed in mutants lacking one

* Corresponding author. Mailing address: Department of Microbiology and Immunology, University of North Dakota School of Medicine, Grand Forks, ND 58202-9037. Phone: (701) 777-2624. Fax: (701) 777-2054. E-mail: kyoung@medicine.nodak.edu.

‡ Present address: Department of Molecular, Cellular and Developmental Biology, Yale University, New Haven, CT 06511.

† Supplemental material for this article is available at <http://jb.asm.org/>.

[∇] Published ahead of print on 4 May 2007.

or more of the AmiABC amidases (5, 22, 23). Also, EnvC may not be required throughout septation because the protein disappears from the septal ring in deeply constricted cells (5). Thus, EnvC seems to function at a very early stage of cell division but is not required near the end.

Gram-negative bacteria divide by circumferential invagination of all three envelope layers (inner and outer membranes and PG), with final septation probably being coincident with the fusion of these layers at a point near the end of the division process. Therefore, since the gram-negative hydrolases seem to be active throughout the invagination process, it is possible that these enzymes perform multiple, overlapping, and potentially sequential functions during cell separation.

While investigating the functions of the murein hydrolases, Heidrich et al. observed that sacculi from *E. coli* lacking three amidases have thick dark bands situated at sites of incomplete septation between adjacent cells (22). The implication is that these novel PG structures accumulate due to a loss of amidase activity, but nothing is known about which amidase is responsible or whether these structures reflect physiologically important stages during the course of septum development. In this work we further characterize the nature and functional import of these PG bands and propose that they represent intermediate stages during septal invagination. The existence, composition, and behavior of these rings suggest that some of the PG hydrolases act sequentially, that they sustain PG synthesis during cell division, that they are required for creating septa of specific geometries, and that they may modify polar PG so that it resists the insertion of new wall materials.

MATERIALS AND METHODS

Bacterial strains, plasmids, and phage. Bacteria and plasmids are listed in Table 1. Bacteria were grown in Luria-Bertani (LB) medium with the following antibiotics as required: ampicillin (50 µg/ml), kanamycin (50 µg/ml), or chloramphenicol (25 µg/ml). Yeast extract and tryptone were from Difco (Detroit, MI). All other chemicals and antibiotics were from Sigma Chemical Co. (St. Louis, MO) or Fisher Scientific (Pittsburgh, PA). Transduction via bacteriophage P1 was performed as described previously (33).

Molecular techniques. Plasmids were isolated using QIAprep spin Miniprep kits (QIAGEN Corp., Valencia, CA) according to the manufacturer's instructions. Competent cells were prepared and transformed by electroporation, using a Gene Pulser apparatus from Bio-Rad (Hercules, CA). Electroporation does not give a high yield for triple amidase mutants, so transformation into these strains was performed by using CaCl₂-competent cells as described previously (45).

Purification of sacculi. Sacculi were prepared as described by de Pedro et al. (16). Cells from 80 to 100 ml of culture were harvested at an optical density at 600 nm (OD₆₀₀) of 0.6 by centrifugation (10,000 × *g*) for 5 min at room temperature, and the pellets were resuspended in 3 ml of LB medium and added dropwise to a tube containing 6 ml of boiling 6% sodium dodecyl sulfate (SDS). The samples were boiled for 3 to 4 h and incubated overnight at room temperature with gentle stirring. Next morning, the tubes were boiled for 1 h, and sacculi were sedimented by ultracentrifugation at 70,000 rpm (Beckman Optima TLX) for 15 min at 30°C. The pellets were resuspended in 2.5 ml of 4% (wt/vol) SDS in a closed tube and incubated in a boiling water bath for 2 h. Sacculi were sedimented as above and washed with 1% SDS. Sacculi were resuspended in phosphate-buffered saline (PBS), treated with α-chymotrypsin (300 µg/ml final concentration), and incubated overnight at 37°C. The sacculi were pelleted as above and resuspended in 1% (wt/vol) SDS, incubated for 2 h in a boiling water bath, and pelleted. The final pellet was dissolved in 100 to 200 µl of distilled H₂O and stored at 4°C.

Labeling sacculi with NHS-Texas Red-X and antibodies. The sacculi suspension was diluted 1:5 or 1:10 in 50 µl of 0.1 M NaHCO₃ buffer (pH 8.0). To this was added 1.5 µl of *N*-hydroxysuccinimide (NHS)-Texas Red-X (1 µg/ml) (Invitrogen-Molecular Probes, Eugene, OR) with vigorous vortexing. The suspension was incubated in the dark for 15 min, and the reaction was stopped by

TABLE 1. *E. coli* strains and plasmids

Strain or plasmid	Genotype or relevant features ^a	Reference or source
<i>E. coli</i> strains		
CS109	W1485; <i>rph rpoS</i>	C. Schnaitman
RP1	CS109; <i>amiC::Kan</i>	40
RP37	CS109; <i>amiA::Cam</i>	40
RP49	CS109; <i>amiB yje25::res</i>	40
RP75	CS109; <i>amiA::Cam amiB yje25::res</i>	40
RP77	RP75; <i>amiC::Kan</i>	40
RP161	CS109; <i>amiA::Cam amiC::Kan</i>	40
RP108	CS109; <i>dacA::res amiA::Cam amiB yje25::res amiC::Kan</i>	40
RP273	CS109; <i>amiB yje25::res amiC::Kan</i>	This work
Plasmids		
pFAD38	SulA expression vector; Amp ^r	2
pGFPuv	pUC19 plus <i>gfpUV</i> ; Amp ^r	BD Clontech Labs
pDSW230	Expressing <i>ftsZ-gfp</i> ; Amp ^r	52
pDSW234	Expressing <i>gfp-ftsI</i> ; Amp ^r	52
pBAD24-IscA ₅₀₇₋₆₂₀	Expressing IcsA ₅₀₇₋₆₂₀ -GFP; Amp ^r	10
pBAD24-IscA _{Δ507-729}	Expressing IcsA _{Δ507-729} -GFP; Amp ^r	10

^a Cam, chloramphenicol.

adding 5 µl of lysine (5 mg/ml stock). The sample was washed once with 0.1 M NaHCO₃ buffer and two times with distilled H₂O by centrifugation at high speed for 10 to 12 min in an Eppendorf MiniSpin microcentrifuge. The pellet was dissolved in 30 to 50 µl of H₂O, and 2 µl was coated onto a glass coverslip and air dried. The coverslip was washed five times with distilled water and five times with PBS containing 0.2% gelatin and 0.5% bovine serum albumin (PBG), after which it was immersed for 1 h in rabbit anti-murein antibody (M. de Pedro, unpublished data) diluted 1:250 in PBG and then washed six to eight times with PBG. The coverslip was then immersed for 1 h in AlexaFluor 488 goat anti-rabbit immunoglobulin G (IgG) antibody (Invitrogen-Molecular Probes) diluted 1:250 in PBG. The slide was washed with PBS and H₂O to remove excess antibody, air dried, and put on a slide with Prolong Gold Antifade reagent (Invitrogen-Molecular Probes). Microscopic observations were performed by using a Zeiss Axio Imager upright microscope fitted with an AxioCam charge-coupled-device camera.

D-Cysteine labeling of PG. From overnight cultures, bacterial strains were diluted 1:100 into LB medium containing 150 µg/ml (final concentration) of D-cysteine (Sigma) and grown with aeration at 37°C to an OD₆₀₀ of 0.6. Cultures were harvested and resuspended in LB medium without D-cysteine. Depending on the need of the experiment, aztreonam (1 µg/ml) was added to the above culture at the start of the chase period. The culture was then allowed to grow for 30 min (chase period), after which the cells were harvested, and sacculi were prepared for biotinylation and immunolabeling.

Biotinylation of purified sacculi. Biotinylation was performed as described by de Pedro et al. (16). In brief, a reduction step was performed to regenerate the thiol groups oxidized during cell growth and sacculus purification. Sacculi were mixed with 450 µl of 0.5 M NaHCO₃ buffer (pH 8.5), 1 mg of NaH₄B was added, and the sample was incubated at room temperature for 30 min. Excess NaH₄B was removed by adding 20% phosphoric acid until the pH dropped to 3. After 5 min, the pH was increased to 8.0 by adding 0.5 M NaHCO₃, followed by the addition of 0.4 ml of a 2.2 mg/ml solution of *N*-[6-(biotin-amido) hexyl]-3'-(2'-pyridyl)dithio) propionamide (biotin-HPDH; Pierce, Rockford, IL) in dimethyl sulfoxide. After 1 h the samples were centrifuged (10 to 15 s at high speed in an Eppendorf centrifuge) to remove the white precipitate formed during the reaction. The supernatant with sacculi was removed and treated with 2.5 ml of H₂O and 50 µl of 6% SDS, after which the sacculi were sedimented by ultracentrifugation. Sacculi were resuspended in 50 µl of H₂O and immunolabeled or stored at 4°C. Immunolabeling was performed by adding anti-biotin mouse IgG (Invitrogen) diluted 1:250 in PBG, which was detected by adding the secondary antibody AlexaFluor 594 goat anti-mouse IgG (Invitrogen) diluted 1:250 in PBG.

TEM analysis of purified sacculi. Formvar/carbon film-coated copper grids (200-mesh; Electron Microscopy Sciences, Hatfield, PA) were floated on an aqueous sacculus suspension and removed, and the sample was air dried on the grids. The grids were washed three times by flotation on drops of distilled H₂O,

floated on a 0.5% bovine serum albumin solution for 5 min, washed with water and stained with 1% uranyl acetate for 1 min, air dried, and observed with a Hitachi 7500 transmission electron microscope (TEM).

Labeling of outer membrane proteins. *E. coli* outer membrane proteins were labeled with NHS-Texas Red-X or NHS-Oregon Green 488-X (Molecular Probes) as described previously (15). In brief, bacteria were grown at 37°C to an OD₆₀₀ of 0.4, harvested, washed with NaHCO₃ buffer (0.1 M, pH 8.0), and stained with NHS-Texas Red-X (2.5 μg/ml) or NHS-Oregon Green (2.5 μg/ml). The stained cells were washed with bicarbonate buffer, resuspended in LB medium, and observed by phase or fluorescence microscopy. Image processing was performed with the ImageJ program (National Institutes of Health, Bethesda, MD), and the average background value of a cell-free area was subtracted from each image.

Inner membrane labeling. The inner membrane was labeled with FM 4-64 (Molecular Probes) as described previously (20). Cultures were grown at 37°C to an OD₆₀₀ of 0.4 to 0.5, harvested by centrifugation, resuspended in filtered LB medium, and labeled with FM 4-64 (final concentration, 4 μg/ml). The suspension was incubated in the dark for 30 min with gentle shaking, and the cells were observed by fluorescence microscopy.

Live-dead staining. Cell viability was determined with a LIVE/DEAD BacLight bacterial viability kit (Invitrogen-Molecular Probes). *E. coli* RP77 was grown overnight at 37°C in LB medium without shaking. To 300 μl of this culture was added 1 μl of SYTO-9:propidium iodide mix in a 1:1 ratio, and the suspension was incubated in the dark for 15 min. Cells were spotted onto an agarose-coated slide and observed by fluorescence microscopy.

Confocal microscopy and FLIP. Fluorescence loss in photobleaching (FLIP) was determined with cells expressing cytoplasmic green fluorescent protein (GFP) from pGFPuv and colabeled with FM 4-64. Cultures were grown at 30°C overnight in LB medium containing ampicillin (50 μg/ml) and 0.2% glucose. Cultures were diluted 1:100 into LB medium plus ampicillin and incubated at 37°C. At an OD₆₀₀ of 0.4, 1 ml of culture was harvested and resuspended in filtered LB medium, labeled with FM 4-64 (4 μg/ml), and incubated in the dark for 30 min. Cells were spotted onto a glass slide coated with LB medium in 1% agarose.

Confocal microscopy was performed with a Zeiss microscope (model LSM510 Meta; Zeiss, Jena, Germany) fitted with a 63× plan-fluar objective (1.45 numerical aperture) and driven by Zeiss AIM software. For FLIP images, sets of cells in chains were selected and photographed. The size of the bleach area was set to the width of a cell (~1 μm), and this area was bleached by 100 to 200 iterations of exposure to the 488-nm line of the argon laser. Because GFP expression differs from cell to cell, the number of iterations was adjusted to obtain complete bleaching. Fluorescence photobleaching was documented by photographing the cells every 10 s, and the images were visualized with the Zeiss LSM image browser and the ImageJ program.

Expression of GFP fusions. Expression of IcsA-GFP fusions was performed as described previously (37). The cells were grown at 30°C in LB medium plus ampicillin (50 μg/ml), and fusion protein expression was induced by adding 0.2% arabinose for 40 min. For GFP-FtsI and FtsZ-GFP expression, cells were grown at 37°C in LB medium plus ampicillin (100 μg/ml) and induced for 40 min with 10 μM isopropyl-β-D-thiogalactopyranoside (IPTG) for GFP-FtsI or 2.5 to 5 μM IPTG for FtsZ-GFP (52). The cells were harvested, and 5 μl was spotted onto agarose coated slides and observed by phase and fluorescence microscopy.

RESULTS

Amidase mutants produce PG rings at incipient septa.

Heidrich et al. created mutants deficient in three amidases, AmiABC, and found that the resulting cells grew as long chains that had thick dark bands of PG between adjacent cells in purified sacculi (22). We refer to these banded structures as PG rings or septal PG (SP) rings, the latter being associated with clearly invaginating septa.

To characterize these structures further, we first confirmed that equivalent PG rings were formed in a different triple amidase mutant, *E. coli* RP77 (Δ amiABC), constructed in the CS109 (*E. coli* W1485) genetic background (Fig. 1A). When sacculi from chains of this mutant were examined by TEM, thickened and dark hoops were visible against a uniform back-

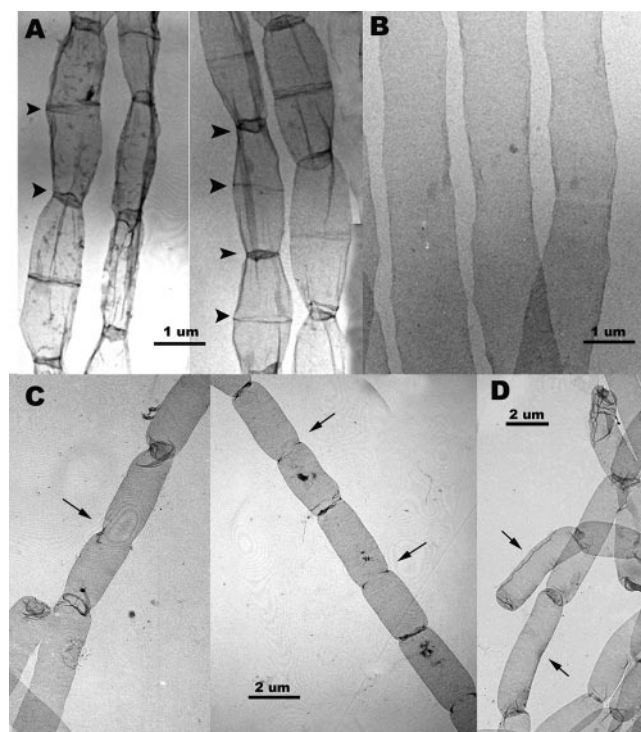


FIG. 1. Cell division is required for development of SP rings in amidase mutants of *E. coli*. Sacculi were prepared and observed by TEM. (A) PG rings in *E. coli* RP77 (Δ amiABC). Arrowheads point to examples of typical PG rings (large-diameter rings at sites with little or no constriction) and SP rings (small-diameter rings located at sites with obvious cell constriction). (B) *E. coli* CS109 forced to grow as filaments in the presence of the PBP3-inhibitor aztreonam. No PG rings are visible, though the cells continued to elongate. (C) *E. coli* RP77 incubated in the presence of aztreonam for 40 min before preparation of sacculi. Although preexisting circular and partial PG rings remain, in the elongated portions of these cells no new rings formed (e.g., arrow in left-hand chain). Also, the continued development of early-stage PG rings at the time of antibiotic addition was aborted (e.g., arrows in right-hand chain). (D) *E. coli* RP77 forced to grow as filaments by inhibiting FtsZ by expressing the *sulA* gene from plasmid pFAD38. SulA production was induced with 0.2% arabinose for 1 h before preparation of sacculi. No new PG rings of any sort are visible within the elongated cells.

ground of more lightly stained PG (Fig. 1A). Because sacculi are thin and fold slightly when attached to the TEM grids, most of these more heavily stained structures were seen to be continuous rings that encircled the cell diameter at sites where cell constriction was obviously in progress (SP rings) as well as at sites where new constrictions would be expected at the onset of cell division (PG rings) (Fig. 1A). In portions of sacculi that had settled more evenly, the structures appeared as a single line (or two parallel lines) extending from one side of the sacculus to the other. These results indicate that PG rings are reproducible structures in different *E. coli* strains. In addition, morphologically similar bands were observed in sacculi from an *amiABC* mutant of *Salmonella enterica* serovar Typhimurium (see Fig. S1 in the supplemental material), suggesting that SP rings are common among this branch of gram-negative bacteria.

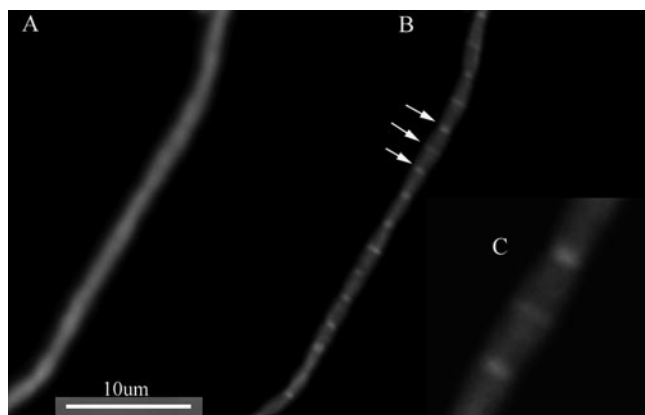


FIG. 2. PG ring detection by staining with NHS-Texas Red-X. (A) The outer surface of sacculi from *E. coli* RP77 was labeled uniformly with anti-murein antibody and AlexaFluor 488-labeled goat anti-rabbit antibody. (B) RP77 sacculi labeled with NHS-Texas Red-X. Heavily labeled PG ring bands appear along the length of the sacculi. Arrows indicate the three rings magnified in panel C. (C) Area from panel B at a higher magnification, showing a large (center) PG ring bracketed on either side by more advanced-stage (smaller) SP rings.

Detection of PG rings by fluorescence light microscopy. To date, PG rings have been visualized only by TEM analysis of isolated sacculi (22; also this work). To corroborate the existence of PG rings via a second method, we devised conditions under which PG rings could be observed by fluorescence light microscopy. Sacculi from *E. coli* RP77 (Δ *amiABC*) were purified and labeled with anti-murein antibody and/or with NHS-Texas Red-X. Because of its large size, anti-murein antibody cannot penetrate the PG network and therefore labels only the surface of bacterial sacculi. On the other hand, NHS-Texas Red-X labels PG by covalently binding to free amino groups in the side chains, and, because of its small size, this molecule can penetrate to the interior of purified sacculi to label PG rings that may not be accessible from the exterior.

PG rings were not visible in sacculi labeled with anti-murein antibody and stained with a secondary AlexaFluor 488-labeled antibody. Instead, these sacculi exhibited uniform fluorescence along their length (Fig. 2A). In contrast, chains of sacculi stained with NHS-Texas Red-X revealed a pattern of regularly spaced bright bands that mirrored the distribution of PG rings, as seen by electron microscopy (Fig. 2B and C), as would be expected if PG rings corresponded to a local thickening of the sacculus. Because TEM identified PG rings at every potential division site in chains of amidase mutants, PG rings stained by NHS-Texas-Red should also be present at regular intervals. Consistent with this expectation, fluorescence intensity profiles exhibited a regular and repeating pattern of NHS-Texas Red-X peaks (data not shown but see Fig. 3G and H), whereas staining of surface murein by anti-murein antibody remained constant along the length of the chain (data not shown). Additional evidence that these bands corresponded to PG rings as observed in TEM was that many of the fluorescent rings were demonstrably smaller in diameter than others (see below), and their sizes followed the normal pattern of constriction along the chain, where one deep constriction was flanked by two shallow ones. Overall, the data are consistent with the interpretation that NHS-Texas Red-X labeling detected PG rings in

this triple amidase mutant. Similar structures were observed after NHS-Texas Red-X staining of the double amidase mutants (data not shown). The results indicate that PG rings can be detected by light microscopy and suggest that they probably represent a thickened rim of PG that may be most easily accessed from the internal surface of the sacculus.

Loss of any two amidases generates PG rings. To determine if deletion of all three amidases was necessary to produce PG rings, we constructed strains lacking each of the individual amidases as well as mutants lacking different pairs of amidases (Table 1). The chaining properties of these mutants were essentially identical to those constructed in a different background by Heidrich et al. (22) (see Table S1 in the supplemental material). Strains lacking a single amidase had 3 to 4 cells per chain, those lacking two amidases had 3 to 14 cells per chain, and the triple amidase mutant grew in chains of 20 to 60 cells (see Table S1 in the supplemental material).

When purified sacculi were visualized by electron microscopy, equivalent darkly stained PG rings were observed at incipient division sites in the triple mutant RP77 (Δ *amiABC*) (Fig. 1A) and in the doubly mutated strains RP75 (Δ *amiAB*) (see Fig. S1F and G in the supplemental material) and RP161 (Δ *amiAC*) (see Fig. S1E in the supplemental material), as well as in strain RP273 (Δ *amiBC*) when visualized by fluorescence microscopy (data not shown). Because a different amidase was active in each of the three double mutants, the fact that PG rings were formed in each case indicates that no single amidase compensated for the loss of the other two. Conversely, since deleting any two amidases produced cells with PG rings, the results indicate that no one amidase was uniquely responsible for the phenotype. However, in the double mutants many constriction sites were deeper, and their associated PG rings were smaller than those observed in the triple amidase mutant, suggesting that cell constriction routinely proceeded further than in the mutant lacking all amidases. PG rings were not observed in mutants lacking any single amidase, presumably because cell constriction and septal development continued to proceed normally even though cell separation was delayed slightly.

Developmental pattern of PG and SP rings. PG rings could represent either a static or a dynamic structure within PG. Because the presence of these rings could be observed only in purified sacculi and not in living cells, we could not monitor the development of a single ring over time. However, a simple developmental scheme could be inferred by inspecting the diameters of PG rings along the length of filaments composed of connected sacculi. In every case, PG rings were arranged in an equivalent pattern: a large-diameter PG ring was always bracketed on either side by two SP rings of smaller diameter, with the diameters of all rings coinciding with the degree of constriction at those sites (Fig. 1A). The alternating pattern was easy to see in TEM micrographs, but the same relationship was also visible in sacculi stained with NHS-Texas-Red and viewed by fluorescence microscopy (Fig. 2C). This repetitive configuration was consistent over long stretches of chained sacculi from the triple amidase mutant. These data suggest that PG rings form at incipient septa during the onset of cell division and that SP rings represent the leading edge of synthesis at each developing constriction site. This interpretation was reinforced by complementary experiments showing that every

performed (older) SP ring was bracketed on either side by two newly synthesized PG rings (discussed below in the section “PG rings exhibit characteristics of inert PG”). In sum, SP rings most likely reflect the existence of a transient PG intermediate that is created during normal cell septation but which is amplified sufficiently to be observed only when multiple amidases are absent.

PG ring formation requires active cell division. Because PG rings were observed at constriction sites and appeared to consist of newly formed SP, it seemed probable that cell division was essential for their formation. To test this possibility, we determined if PG rings appeared in sacculi of wild-type *E. coli* in which cell division was interrupted. The FtsZ protein regulates the timing and positioning of the divisome (12, 21) and can, even in the absence of downstream division proteins, initiate septal constriction to produce an early form of PG (35, 53). To see if PG ring formation in amidase mutants depended on this early stage of cell division, we inhibited FtsZ by overproducing the SulA protein (an FtsZ inhibitor) (34, 51) in the triple mutant RP77. Sacculi from these cells were elongated and connected in chains, but no PG rings were visible at sites where division would be expected to occur (Fig. 1D), confirming that FtsZ was required for PG ring formation. In addition, these sacculi showed no evidence of constriction furrows, consistent with the absence of FtsZ (Fig. 1D).

Since PG ring formation required the initiation of cell division, the next question we addressed was whether rings were produced by the synthesis of normal SP. Division was inhibited in the parental strain CS109 by adding the antibiotic aztreonam, which targets the essential division protein PBP3 (FtsI) and interrupts SP synthesis (3, 24). The resulting smooth filamentous sacculi contained no rings, either in TEM micrographs (Fig. 1B) or in NHS-Texas Red-X-stained sacculi (not shown), indicating either that PG ring formation required active PBP3 or that the wild-type amidases still present in the parental strain had removed the early ring forms. To discriminate between these alternatives, we inhibited PBP3 by adding aztreonam to the triple amidase mutant RP77 (Δ amiABC), which normally forms chains of cells separated by PG rings. If PG ring formation was driven by PBP3-mediated synthesis, then individual cells in chains of this mutant should elongate (because cell division was inhibited), but no new PG rings should form (because PBP3 was inhibited). Consistent with this prediction, when RP77 was incubated for 40 min in the presence of aztreonam, each cell in the chain elongated, but no new PG rings were observed at locations representing potential or newly initiated division sites (Fig. 1C). In some cases, elongating cells were evidently caught at an early stage of septal development so that remnants of preformed PG rings persisted (Fig. 1C, right-hand chain). Interestingly, many sacculi exhibited shallow constriction furrows at the centers of elongated cells, even though complete PG rings were not present at these sites (Fig. 1C, left-hand chain). Thus, even in the presence of aztreonam, which should inactivate the bulk of PBP3, the cell could initiate divisome assembly, mark the division site, and initiate the earliest stage of cell constriction. The results confirmed that PG ring formation required the initial stages of cell division, initiated by FtsZ, as well as PG synthesis as promoted by PBP3 or that of another protein whose activity depended on PBP3.

PG rings exhibit characteristics of inert PG. The preceding results suggest that PG rings represent one or more stages in the development of future poles. One of the hallmarks of mature poles is that they are inert; that is, polar PG is not diluted by the insertion of new material, nor is it removed appreciably by recycling (16, 17, 32). However, it is not known when PG begins to display these characteristics. Does SP become inert as soon as it is synthesized, or is inertness imparted only after constriction and pole formation are complete? Because PG rings appear to represent the leading edge of septal synthesis, we performed D-cysteine pulse-chase experiments to determine when PG in these rings became inert.

PG from *E. coli* RP77 (Δ amiABC) was labeled uniformly by growing cells in the presence of D-cysteine, and the locations of newly inserted PG were marked by growing the cells for an additional 30 min in the absence of this amino acid. Residual D-cysteine residues were detected in purified sacculi by biotinylation followed by immunolabeling with an AlexaFluor 594-conjugated (red) secondary antibody (16). PG rings were visualized by labeling these same sacculi with NHS-Oregon Green. In this procedure, newly incorporated PG is nonbiotinylated and appears as dark unstained areas in a background of red prechase (older) PG, and PG rings appear as heavily stained green bands set against a uniformly labeled background of lighter green.

Because the appearance of new PG rings required active cell division, we blocked division by adding aztreonam during the chase period to observe the fate of preformed PG rings. No new PG rings should form in such cells because PBP3 is inhibited, so that any rings observed in the resulting chains would have been constructed prior to the chase period. Consistent with this expectation, no PG rings (green bands) were present in D-cysteine-free (dark) regions where the label had been removed due to new PG synthesis during the chase (Fig. 3D to F and H). Conversely, if preformed PG rings became inert during or very quickly after synthesis, then the rings should retain the D-cysteine label. Consistent with this prediction, these PG rings remained unchanged after division was inhibited; the (green) rings retained their D-cysteine label (red) throughout the chase period (Fig. 3D to F and H). This result was visualized more quantitatively by inspecting the distribution of labeled material in fluorescence intensity profiles produced by scanning along the length of the cell chains (Fig. 3H). Wherever there was a preformed PG ring (green peak), there was also a concomitant spike of D-cysteine-containing material (red peak) (Fig. 3H, red arrows). These data indicated that, once differentiated, PG rings incorporated no (or very little) new PG, suggesting that these structures behaved as though composed of inert PG.

A limitation of the preceding experiments is that if new PG incorporation into PG rings is accomplished only by PBP3-directed synthesis during septation, then it would not be surprising that PG rings behaved as though inert when PBP3 was inhibited. To rule out this possibility, we examined the composition of PG rings in division-proficient cells. In pulse-chased sacculi of *E. coli* RP77 (Δ amiABC), PG rings were observed in darkened areas, where D-cysteine label was lost during the chase, as well as in red areas, where D-cysteine label was retained (Fig. 3A to C and G). PG rings in D-cysteine-free (dark) zones indicated that the rings were composed of new PG pre-

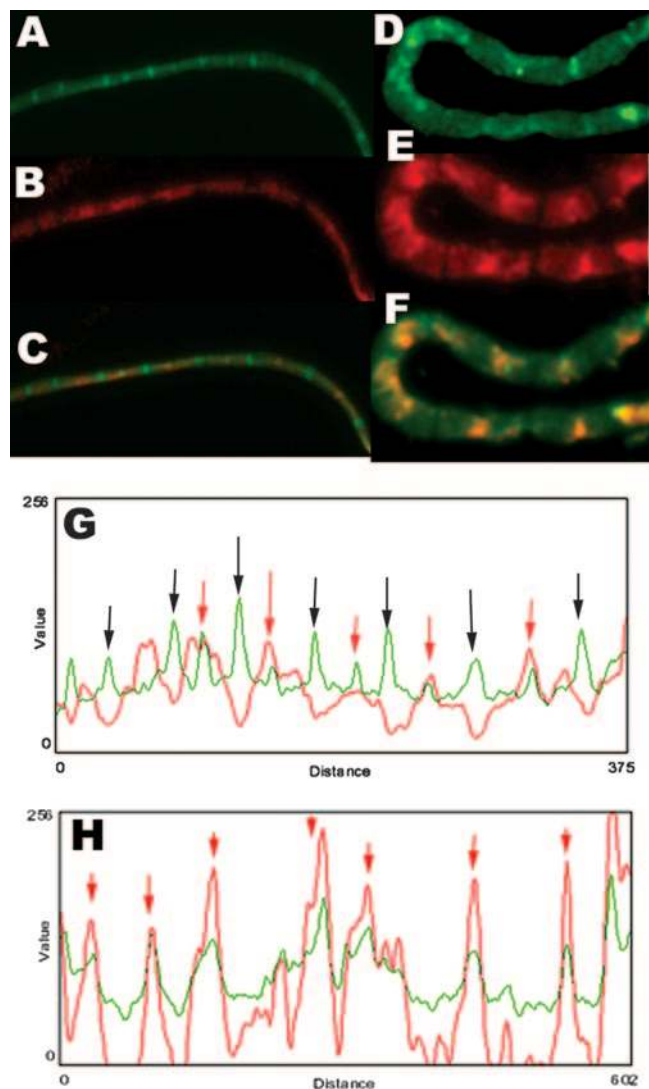


FIG. 3. PG rings behave as though composed of inert PG. *E. coli* RP77 (Δ *amiABC*) was grown at 37°C in LB medium containing D-cysteine and then shifted to grow an additional 30 min in D-cysteine-free medium without (A to C and G) or with (D to F and H) the antibiotic aztreonam (1 μ g/ml). Sacculi were stained with NHS-Oregon Green and also with anti-biotin mouse primary antibody followed by AlexaFluor 594-labeled goat anti-mouse secondary antibody. (A) Oregon Green-stained sacculi. PG rings are visible as brightly fluorescent bands along the length of the sacculus chain. (B) Location of newly incorporated PG. Older (D-cysteine-containing) PG stains red, while newly synthesized PG (D-cysteine-free material incorporated during the chase period) is unstained (dark areas). (C) Merged image of panels A and B. PG rings present in newly synthesized PG are green, while PG rings in preexisting PG are yellow. (D) Sacculi forced to grow as filaments in the presence of aztreonam and then stained with Oregon Green. PG ring material is more highly fluorescent. (E) Location of newly incorporated PG in sacculi forced to grow as filaments in the presence of aztreonam. Older (D-cysteine-containing) PG stains red, while newly synthesized PG (D-cysteine-free material incorporated during the chase period) is unstained (dark areas). (F) Merger of panels A and B. PG ring material (yellow) is almost exclusively localized in areas of preexisting PG. (G) Fluorescence intensity profiles of sacculi in panels A and B. The two profiles display the distribution of preexisting (red) and newly incorporated (green) PG along the length of the chain of sacculi. Black arrows indicate the location of PG rings that actively incorporated new PG, defined as ring positions that exhibit a low-intensity red trace coupled with a high-

intensity green trace. Red arrows indicate the location of PG rings composed of inert PG, defined as ring positions that exhibit high intensity peaks in both the red and green traces. (H) Fluorescence intensity profiles of sacculi in panels D and E. Red arrows indicate the location of PG rings composed of inert PG (ring positions with high-intensity peaks in both the red and green traces). No PG rings incorporated new PG, as denoted by the absence of PG rings with a low-intensity red trace coupled with a high-intensity green trace.

intensity green trace. Red arrows indicate the location of PG rings composed of inert PG, defined as ring positions that exhibit high intensity peaks in both the red and green traces. (H) Fluorescence intensity profiles of sacculi in panels D and E. Red arrows indicate the location of PG rings composed of inert PG (ring positions with high-intensity peaks in both the red and green traces). No PG rings incorporated new PG, as denoted by the absence of PG rings with a low-intensity red trace coupled with a high-intensity green trace.

intensity green trace. Red arrows indicate the location of PG rings composed of inert PG, defined as ring positions that exhibit high intensity peaks in both the red and green traces. (H) Fluorescence intensity profiles of sacculi in panels D and E. Red arrows indicate the location of PG rings composed of inert PG (ring positions with high-intensity peaks in both the red and green traces). No PG rings incorporated new PG, as denoted by the absence of PG rings with a low-intensity red trace coupled with a high-intensity green trace.

intensity green trace. Red arrows indicate the location of PG rings composed of inert PG, defined as ring positions that exhibit high intensity peaks in both the red and green traces. (H) Fluorescence intensity profiles of sacculi in panels D and E. Red arrows indicate the location of PG rings composed of inert PG (ring positions with high-intensity peaks in both the red and green traces). No PG rings incorporated new PG, as denoted by the absence of PG rings with a low-intensity red trace coupled with a high-intensity green trace.

intensity green trace. Red arrows indicate the location of PG rings composed of inert PG, defined as ring positions that exhibit high intensity peaks in both the red and green traces. (H) Fluorescence intensity profiles of sacculi in panels D and E. Red arrows indicate the location of PG rings composed of inert PG (ring positions with high-intensity peaks in both the red and green traces). No PG rings incorporated new PG, as denoted by the absence of PG rings with a low-intensity red trace coupled with a high-intensity green trace.

intensity green trace. Red arrows indicate the location of PG rings composed of inert PG, defined as ring positions that exhibit high intensity peaks in both the red and green traces. (H) Fluorescence intensity profiles of sacculi in panels D and E. Red arrows indicate the location of PG rings composed of inert PG (ring positions with high-intensity peaks in both the red and green traces). No PG rings incorporated new PG, as denoted by the absence of PG rings with a low-intensity red trace coupled with a high-intensity green trace.

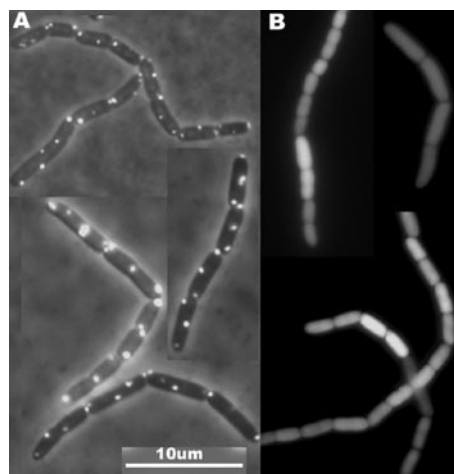


FIG. 4. Poles and incomplete septa of amidase mutants attract IcsA-GFP. *E. coli* RP161 (Δ amiABC) was grown at 30°C in LB-ampicillin medium, production of IcsA-GFP variants was induced by adding 0.2% arabinose for 40 min, and the resulting chains of cells were visualized by fluorescence microscopy. (A) IcsA₅₀₇₋₆₂₀-GFP, a fusion protein that attaches specifically to cell poles, localizes to complete and incomplete septa in cell chains of the double amidase mutant. (B) Diffuse cytoplasmic localization of IcsA_{Δ507-729}-GFP, a variant protein from which polar localization signals have been removed.

The hybrid protein IcsA consisting of residues 507 to 620 and fused to GFP (IcsA₅₀₇₋₆₂₀-GFP) contains a localization sequence that directs the protein specifically to the poles in *E. coli* (10). When expressed in *E. coli* RP161 (Δ amiABC), IcsA₅₀₇₋₆₂₀-GFP protein formed fluorescent foci at the incomplete poles of each cell in the chain as well as at the center of those cells in which a new division septum had only begun to form (Fig. 4A). The control, IcsA_{Δ507-729}-GFP, which lacks the polar localization sequence (10), did not accumulate at the poles or at midcell, but, instead, was present as a diffuse fluorescence within the cytoplasm (Fig. 4B). The results establish that in these mutants nascent septa attracted IcsA-GFP at all stages of cell constriction, a characteristic associated with mature (inert) cell poles. Furthermore, incipient septa developed this ability significantly in advance of the completion of cell constriction, so that IcsA-GFP bound to sites where constriction was moderately advanced as well as to sites where PG ring formation had probably just commenced (i.e., at sites where new septa were in the earliest stages of formation). The most straightforward interpretation of the collective results is that immediately after being synthesized, or very soon afterwards, PG rings become inert and proficient for attracting pole-localized proteins.

Cells in chains are compartmentalized even though PG constriction is incomplete. *E. coli* divides by constriction, and the completion of constriction usually coincides with the final separation of the cytoplasmic compartments of daughter cells. However, as shown here and elsewhere (22, 23), mutants lacking two or three amidases cannot complete cell constriction, and so the daughters remain linked to one another in chains of incompletely constricted cells. Under normal circumstances the three components of the gram-negative cell envelope (inner membrane, PG, and outer membrane) invaginate simultaneously. However, the interruption of constriction in these

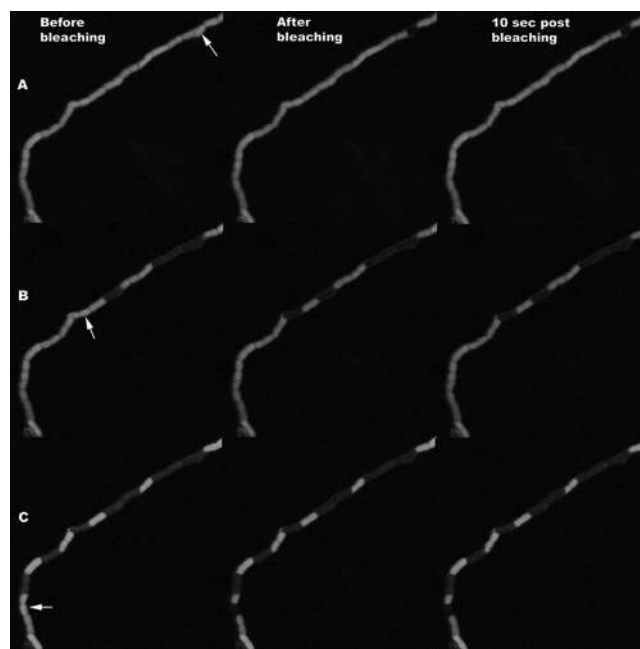


FIG. 5. Cytoplasmic compartmentalization between cells in chains of *E. coli* lacking AmiABC. A cytoplasmic form of GFP was expressed from plasmid pGFPuv in *E. coli* RP77 (Δ amiABC), and the cells were labeled with FM4-64 to stain the inner membrane. Cells were prepared for confocal microscopy, and potential connections between cells were tested by the technique of FLIP. The size of the area to be bleached (indicated by arrows) were exposed to a beam of 488-nm light from an argon laser. A chain was selected, and individual cells (A, B, and C) were bleached in sequence. Cells were photographed immediately before, immediately after, and 10 s after bleaching (columns from left to right). Fully compartmentalized cells were those whose neighbors retained their fluorescence (A and C), while cells that were not compartmentalized were identified as those where fluorescence disappeared from one or more neighboring cells (B).

mutants led us to ask whether invagination had been impaired and whether cells in these chains behaved as individual entities or as though they were connected by a continuous cytoplasm.

To determine if the cytoplasm was continuous between adjacent cells, we expressed a cytoplasmic version of GFPuv in various amidase mutants and monitored the distribution of the protein by using the technique of FLIP. By means of confocal microscopy, one cell in a chain was exposed to a high-intensity laser beam sufficient to bleach away its internal fluorescence. Cells on either side of this bleached cell were monitored to see if their internal fluorescence remained high or decreased. If the two cells were separated by a membranous barrier, fluorescence in the neighboring cell would remain high because GFPuv in that cell could not diffuse across the boundary to be bleached along with GFPuv in the original cell. Alternatively, if the cytoplasm of the two cells was connected, GFPuv in the neighboring cell would diffuse into the bleaching target area, thereby decreasing the fluorescence intensity in the cytoplasm of the second cell.

FLIP was performed on every other cell in chains derived from the amidase mutant RP77 (Δ amiABC) (Fig. 5). In the examples shown, two cells near each end of the chain were compartmentalized; that is, their cytoplasmic contents were

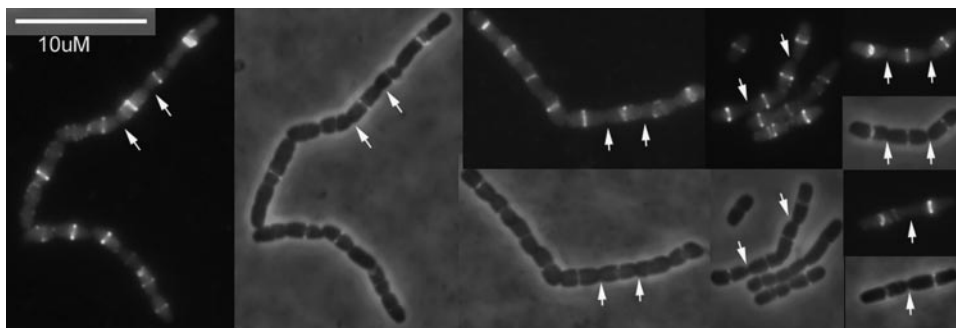


FIG. 6. FtsZ rings do not persist at older division sites in amidase mutants. *E. coli* RP75 (Δ *amiAB*) containing plasmid pDSW230 was grown in LB medium at 37°C to an OD₆₀₀ of 0.2, and IPTG (5 μ M final concentration) was added to induce expression of *ftsZ-gfp*. After 1 h cells were collected for microscopy and examined by phase-contrast and fluorescence microscopy. Representative chains of cells are presented as pairs of photographs, the first showing the location of FtsZ-GFP (fluorescence only) and the second showing the merged phase and fluorescence photos. Arrows indicate septation sites that have no associated FtsZ-GFP ring.

separate as evidenced by the fact that bleaching the neighbors did not decrease fluorescence in these terminal cells (Fig. 5A and C). On the other hand, cells in the interior of the chain were not compartmentalized, because bleaching a cell drastically decreased the fluorescence of one of its immediate neighbors (Fig. 5B). Even so, in these cases there remained a modicum of compartmentalization because, in most chains, no more than two cells shared a common cytoplasm (see Table S2 in the supplemental material). Out of 77 bleaching events in strains lacking two and three amidases, 35% (range, 31 to 39%) were compartmentalized as single cells, 57% (range, 54 to 62%) were doublets in which the cytoplasm of two cells was connected, and only 8% (range, 7 to 10%) represented instances in which the cytoplasm of more than two cells was contiguous (see Table S2 in the supplemental material). The results were similar when FLIP was performed on chains of the triple amidase mutant RP77 (Δ *amiABC*) or on those derived from the double amidase mutants RP161 (Δ *amiAC*) or RP75 (Δ *amiAB*) (see Table S2 in the supplemental material). Thus, even though complete PG constrictions were rarely (if ever) observed in sacculi from these mutants, cytoplasmic compartmentalization still occurred in more than 90% of these cells.

Because complete septal constriction occurred so infrequently in amidase mutants, the only mechanism by which compartmentalized cells could arise would be for the inner membrane to close independently of the PG, thereby creating a barrier between neighboring cells. This event could occur spontaneously, or else the FtsZ-ring could continue to constrict and draw the inner membrane closed. As a preliminary method of distinguishing between these alternatives, we observed the distribution of an FtsZ-GFP fusion protein in these cells. Although FtsZ-GFP assembled into complete rings or spirals within the chains of *E. coli* RP75 (Δ *amiAB*), no clearly advanced constriction rings were formed (Fig. 6). Instead, a large number of cells (~23%) had no FtsZ-GFP ring at the medial constriction (the old division site) but had FtsZ rings at one or both quarter positions (the new division sites) (Fig. 6). It seemed possible, then, that FtsZ rings at older, but incompletely constricted, division sites had continued to contract and pull the inner membrane closed so as to separate the cytoplasm between daughter cells (cytokinesis), after which the FtsZ migrated to new division positions. This scenario could be true

only if at least some FtsZ rings constricted completely in the amidase mutants. To test this possibility, we monitored the behavior of FtsZ-GFP by time-lapse photomicroscopy in the triple amidase mutant RP77 (Δ *amiABC*) and found that at least some FtsZ rings did constrict (not shown). Thus, even though amidase mutants were unable to complete normal septation of all three envelope layers, it appeared that invagination of the inner membrane could be completed independently, perhaps driven by constriction of the divisome ring. However, this process did require that an early phase of invagination be completed because cell filaments created by inhibiting PBP3 with aztreonam exhibited no compartmentation in the FLIP procedure (not shown).

Amidase mutants produce abnormal septa. Amidase mutants lacking PBP5 form twisted chains having abnormal “saddle joint” cell junctures (40). One of the mechanisms by which this might occur would be if septum geometry were altered so that the cells divided at odd angles relative to one another. To see if this was true, we stained live cells with NHS-Oregon Green (to label the outer membrane) or with FM4-64 (to label the inner membrane) in order to visualize the geometric arrangement of septa between cells in chains of the triple amidase mutant RP77 (Δ *amiABC*) and its PBP5-deleted derivative RP108 (Δ *amiABC* Δ PBP5) (Fig. 7A and B). In both strains, cell chains contained numerous septa that were tilted relative to the side walls instead of bisecting the cells at a 90° angle (Fig. 7A and B, arrows). Interestingly, in many cases pairs of successive septa were slanted in opposite directions relative to one another (Fig. 7A and B), which would seem to rule out a simple explanation based on the symmetric placement of septa as directed by the Min protein system (44). Although the triple amidase mutant RP77 had many tilted septa, *E. coli* RP108, which lacked PBP5 in addition to *AmiABC*, formed twisted chains and exhibited an even greater number of abnormal septa (Fig. 7 and data not shown). These results indicate that amidase activity is required for the proper orientation of septa between dividing cells and that the loss of PBP5 exacerbates these distortions in septal geometry. Similarly, tilted septa were observed by following the localization of a GFP-FtsI fusion protein at division sites in *E. coli* RP77 (Fig. 7C). Here also a number of GFP-FtsI rings were angled or located imperfectly (Fig. 7C).

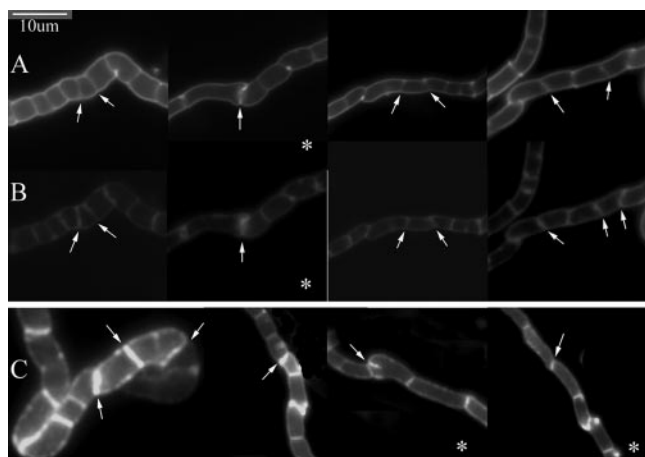


FIG. 7. Abnormal septa in amidase mutants. Cultures of *E. coli* RP77 ($\Delta amiABC$) (marked with an asterisk) and *E. coli* RP108 ($\Delta amiABC \Delta PBP5$) (unmarked) were stained to visualize septal cross-walls. (A and B) Paired representative chains stained with NHS-Oregon Green 488-X to label the outer membrane (A) or with FM4-64 to label the inner membrane (B). (C) Chains of cells producing GFP-FtsI from plasmid pDSW234. Arrows indicate some of the abnormal septa that are visibly misshapen or tilted relative to the longitudinal axes of the chains.

Cell chains probably propagate by intrachain death or lysis.

Rough estimates of the time required to complete a single division event can be calculated by considering the mean chain lengths produced by the amidase mutants. The observed chain length for double mutants is consistent with a four- to eightfold increase in the time per division event (data not shown). The mutant lacking all three amidases would require the equivalent of four to five doubling times to complete a single septation event (data not shown). This latter figure is greater than the cultivation time in most of our experiments, so these cells may not divide at all during the observational period. Therefore, a lingering question is why the different mutants produce chains of different lengths if the cells of which they are composed cannot complete constriction or separation (in the case of the triple mutant) or do so only very slowly (in the case of the double mutants).

The two simplest answers to the above question seem to be that either (i) constriction sometimes goes to completion so that one cell chain becomes two or (ii) cells internal to a chain may randomly die or lyse and break long chains into shorter fragments. While performing the FLIP experiments described above, we observed a significant number of dead cells in cultures of *E. coli* RP77 ($\Delta amiABC$). When cells were examined further by live/dead staining, a majority of dead cells were found at the ends of these chains (see Fig. S2 in the supplemental material). Of 100 chains examined, 87% presented with dead cells at both ends (21%) or at one end (32%) or else had dead cells at the chain ends as well as one or more dead cells internal to the chain (34%). In only 13% of the chains could we see no dead cells at either end, and even in these there were many cases in which it appeared that the final live cell in the chain was attached to the broken remnants of a cell that remained unstained. In addition, the distribution of dead cells at chain ends was highly skewed. Out of 3,397 cells examined in

chains averaging 40 cells long, 519 (15%) were dead; and of the dead cells, 57 (11%) were found at chain ends while the rest were at internal positions. If dead cells had been distributed randomly among the 170 chain ends, then 6.5% (11 of 170) should have consisted of a dead cell. Instead, dead cells were present at 38% (57 of 170) of the chain ends. The surplus strongly suggests that the visible chains were generated from longer chains by the death and breakage of cells rather than by a delayed cell separation.

Although the results argue in favor of chain breakage being the major method for propagating chains of amidase mutants, we cannot rule out the possibility that some septa go to completion and reduce chain length. In fact, we favor this interpretation for mutants lacking a single amidase and at a low frequency in cells missing two amidases. However, in mutants lacking three amidases, it appears very likely that chains fragment not by natural cell division but by the random death of cells within chains. This has important implications for interpreting the behavior and roles of other genes that may be deleted from these types of mutants, because chain length may increase if the genes being tested affect either cell separation or the frequency of cell death. When cell chains reach a certain length, more specific experiments will be required to distinguish between these two possibilities.

DISCUSSION

The growing body of evidence that most PG hydrolases are nonessential for normal bacterial elongation has refocused the question of their physiological roles. There are four major alternatives, not mutually exclusive: they may be responsible for separating daughter cells after division is complete, they may be necessary for continued PG synthesis during septation, they may help coordinate outer membrane invagination with septal ingrowth, or they may be required to insert macromolecular structures into or across the cell envelope. At present, the first of these has the most experimental support, particularly with regard to their actions in the gram-positive bacteria (9, 13, 38, 46, 55) and in *E. coli* (22, 23, 40), and the fourth is the least substantiated. In this work we present evidence that at least one type of hydrolase, the murein amidases, is necessary for continued incorporation of PG into the developing septum in *E. coli*. In addition, our results are consistent with the amidases playing an essential part in the recently described Tol-Pal model for the coordinated invagination of the gram-negative envelope (18).

SP rings are scars of incomplete invagination. In gram-negative bacteria the FtsZ protein initiates septation, after which the sequential operation of a set of division proteins creates a mature septum (8, 12, 21). Uniform circumferential invagination of the cell wall seems to be driven by constriction of the divisome ring and is accompanied by PBP3-dependent PG synthesis. An open question is whether this synthesis is equivalent to that which occurs during cell elongation, albeit reoriented to occur in a different plane. Currently, the major role for PG hydrolases is thought to be that of cleaving the PG wall between daughter cells so that they can be separated, a process that may occur either during the invagination process or after septal constriction is completed. Although the actions

of the hydrolases do produce this result, they may do so in a more complicated manner than is currently visualized.

Heidrich et al. concluded that PG-containing septa are formed but not cleaved in mutants lacking the AmiABC amidases, implying that in most cells (95 to 99%) constriction goes to completion but that daughter cells remain attached to one another by a common PG wall (22, 23). However, although the figures presented by Heidrich et al. (and our FLIP results) definitely show that an inner membrane separates many daughter cells, it is not clear that these structures also contain fully formed SP. Instead, our observations suggest that cells in chains are very rarely separated by a wall of unbroken PG even though most cells are compartmentalized, indicating that extensive cytokinesis occurs. This conclusion is also supported by the fact that *E. coli* mutants lacking multiple hydrolases incur significant death rates during long-term culture (e.g., after 3 days in liquid culture or after 2 weeks on agar plates at 4°C) (23). Such a phenomenon is readily understandable if cells in these chains are not fully separated by PG walls so that random lysis of one cell unit would lead to the death of many cell equivalents. Consistent with this expectation, we routinely observed long contiguous strings of dead cells in chains (e.g., see Fig. S2 in the supplemental material). The results suggest that the characteristic features of sacculi from amidase mutants are most easily explained by the existence of incompletely constricted PG at sites of developing septa, which are visualized as thickened and dark bands between daughter cells (SP rings). Indeed, Heidrich et al. (23) appear to have captured just such a ring in thin section within a “wavy septum” between two cells. Near the lateral walls, between the apposed membranes at either end of the septum, there are thick rigid ingrowths that probably represent the “rim” of SP that comprises an SP ring (see Fig. 4b in reference 23). The differences between our results and those of Heidrich et al. (23) with regard to the extent of PG invagination are likely due to our use of purified sacculi instead of whole cells to visualize the state of PG in these mutants.

Because septal ingrowth in *E. coli* normally proceeds by circumferential constriction, the simplest interpretation is that SP rings are the remnants of incomplete septa whose synthesis was stalled at intermediate stages of invagination. New cell wall precursors are incorporated into the “leading edge” of the constricting septal ring (53). Under normal circumstances, amidases cleave this structure so rapidly that PG density at the leading edge is the same as that in other sections of the wall. In fact, no overtly visible differences appear at septal sites in wild-type sacculi of *E. coli*. However, it seems that the absence of two or more amidases retards this hydrolytic processing step but allows PG synthesis to continue, so that, at least for a time, hydrolysis lags behind synthesis. Because of this, constriction is slowed or comes to a halt, and a section of denser PG accumulates and becomes visible as an SP ring. Consistent with this interpretation is the fact that inhibiting cell division abolishes the appearance of new SP rings. Thus, it is likely that SP rings are the visible remnants of one or more intermediate stages of PG synthesis during cell division.

The presence of SP rings suggests the important additional conclusion that ongoing septal constriction depends on PG hydrolysis, even though the two activities may be separated in space. In the absence of hydrolases PG synthesis slows and

eventually stops, inhibiting further constriction, and the sacculi of the two daughter cells remain connected by a thickened band of PG at the division site. Therefore, the relationship between synthesis and hydrolysis need not always be as close as that envisioned in the “multienzyme complex” hypothesis, where the two activities are intimately connected by direct protein-protein interactions (26). Instead, the activities can be uncoupled so that incorporation continues for a short distance beyond the point where septal splitting stops. The relationship is not simultaneous but sequential. Nevertheless, PG hydrolysis behind the leading edge of the septum is required for continued synthesis at the leading edge, and interruptions at this point would leave a visible SP ring in purified sacculi. This situation in *E. coli* contrasts with that in gram-positive bacteria, where a complete septum can be synthesized, but not split, in the absence of hydrolases.

Septal invagination: a hierarchy of hydrolases? All types of PG hydrolases (amidases, endopeptidases, and lytic transglycosylases) have been implicated in splitting the septum to separate *E. coli* cells during cell division (22, 23, 40). For example, among the hydrolase mutants known to have deficiencies in cell separation are those that lack *envC* (5), those that lack *amiC* or *amiABC* (22), those that lack three to six lytic transglycosylases (22, 23), and those that are missing amidases and PBPs (40). Combinations of these mutations significantly increase separation deficiencies, so that up to 100% of the culture may be comprised of chains from 20 to 100 cells in length (23). The involvement of so many different enzymes and the existence of SP rings provoke the speculation that an ordered sequence of hydrolytic events may be required for invagination leading to cell separation. It is not yet possible to clearly distinguish the different stages at which the amidases act. However, since *EnvC* mutants form chains with shallow invaginations, *AmiABC* apparently acts after this initial phase. *AmiC* is distributed diffusely in the periplasm but moves to the septal ring after the *FtsN* protein joins the divisome (4), suggesting that *AmiC* acts later than does *EnvC* (5). This also seems to be true for *AmiA* (and perhaps *AmiB*), which, though diffuse in the periplasm throughout the division cycle, can still substitute for the loss of *AmiC* during invagination and cell separation (4). In line with these observations and data regarding SP ring formation, we propose a simple preliminary pathway for some of these hydrolases, as described in Fig. 8A. In this view, *EnvC* acts early to initiate septal hydrolysis (Fig. 8A, step 1), *AmiC* is the main hydrolase that completes the process of invagination and separation, and *AmiA* and *AmiB* can substitute in the absence of *AmiC* (Fig. 8A, steps 2 and 3). In the absence of two or more amidases, invagination stalls (Fig. 8A, step 4) but *FtsZ* constriction and cytokinesis can still occur, at least in some cases (Fig. 8A, step 5).

Cytokinesis, SP rings, and Tol-Pal-directed invagination. The current feeling is that in the normal course of events the diameter of the *FtsZ* (septal) ring grows smaller and pulls all three layers of the gram-negative cell envelope inwards. In this view, constriction during cell division is a by-product of cytoplasmic motor forces. An alternative is that inward-directed PG synthesis at the division site might aid constriction by “pushing” the inner membrane toward the interior of the cell. If so, then any *FtsZ* rings at this interface would become smaller as a matter of course. Removing multiple amidases

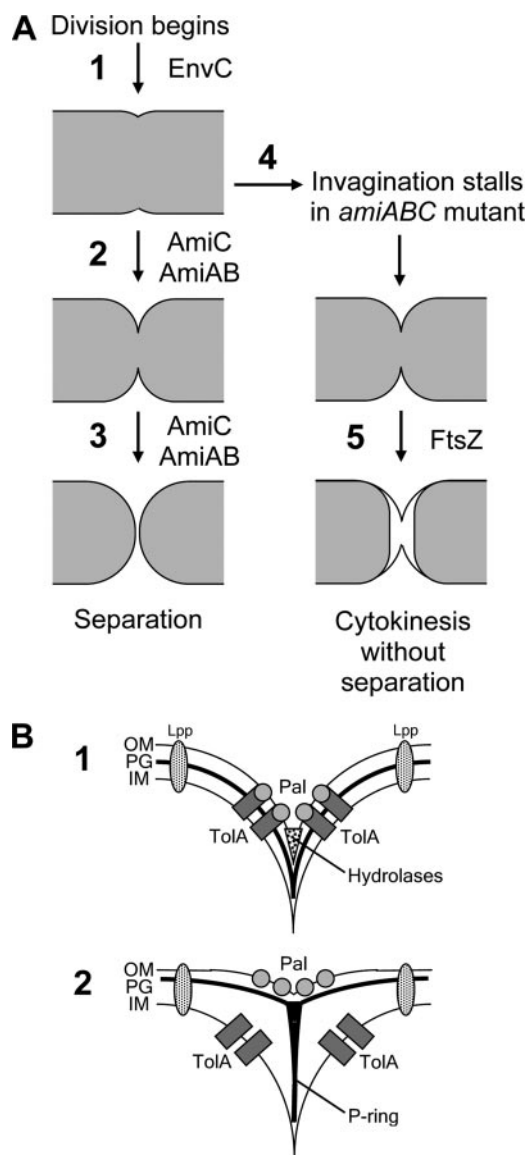


FIG. 8. Schematic models of murein hydrolase activity during septation in *E. coli*. (A) Proposed sequence of hydrolase functions during septal invagination. (B) Invagination of the outer membrane during division in the presence (1) or absence (2) of murein hydrolases. Details are presented in the text.

decouples the invagination process, in that invagination of the inner membrane can continue even if there is not complete invagination of PG and the outer membrane (23; also this work). Taken by itself, this would imply that cell wall synthesis is not essential for cytokinesis in *E. coli*. However, when SP synthesis is inhibited completely by inactivating PBP3, then the FtsZ ring does not close, and the inner membrane does not invaginate. This indicates that, at least in its earliest stages, cytokinesis requires something more than constriction of the FtsZ-dependent divisome. Thus, it seems quite possible that cell division leading to cytokinesis requires a short period of PG synthesis (and perhaps hydrolysis), after which constriction of the FtsZ ring is sufficient for completing invagination of the inner membrane. The possibility of such a PG “checkpoint”

has been suggested by Goehring and Beckwith, who also review evidence pertaining to the decoupling of PG ingrowth and membrane invagination in the gram-positive bacteria (21).

The preceding observations and conclusions fit nicely into a recently advanced scheme for coordinating the invagination of the gram-negative envelope. Gerding et al. find that five proteins of the Tol-Pal complex accumulate at the division septum, and these authors propose a “ratchet” model in which an inner membrane protein (TolA) binds reversibly to an outer membrane lipoprotein (Pal) in a recurring sequence that pulls the outer membrane inwards with the septum as constriction proceeds (18) (schematized in Fig. 8B, diagram 1). In the absence of this system, the outer membrane fails to invaginate smoothly, the volume of periplasmic space at the division site increases dramatically, and patches of outer membrane over the septum balloon outward and pinch off to form independent vesicles (18).

The point to be made here is that the Tol-Pal model includes a central role for hydrolases that split SP as invagination progresses. Thus, if septum splitting does not occur rapidly enough (e.g., if the amidases do not function properly), the inner membrane-embedded PG synthetic machinery can continue to constrict until the periplasmic domain of TolA is drawn so far inwards with the inner membrane that it can no longer interact with Pal in the outer membrane (Fig. 8B, diagram 2). The results reported here are consistent with such an interpretation. When sufficient numbers of murein hydrolases are deleted from *E. coli*, invagination (and PG synthesis) continues for a brief period, but septum splitting is delayed or aborted, thereby producing a ring of thick, unsplit PG at the developing division site (Fig. 8B, diagram 2). These structures would be the SP rings in purified sacculi.

What happens to the FtsZ ring and its associated divisome after SP synthesis stalls? First, FtsZ may abandon the incomplete septum and move to newly formed division sites without constricting so that the inner membrane does not close (e.g., cytokinesis does not occur). That is, once constriction stalls, FtsZ monomers in the original ring may depolymerize and be titrated away. Second, FtsZ may continue to constrict, pulling the inner membrane inward to close (cytokinesis occurs), after which FtsZ moves to new division sites. Third, FtsZ may constrict partially (to a smaller ring), at which point the inner membrane self-seals (cytokinesis occurs), and FtsZ moves to new sites. For example, in short chains of *E. coli envC* mutants, 40% of the cell pairs have a visible septal constriction but do not have an associated ZipA-GFP ring, and in 38% of cell pairs the septal ring disappears and reappears at one or both sites of future septation (5). Both behaviors reflect the premature disassembly of septal rings. Our time-lapse observations of FtsZ-GFP favor continued constriction, but the low sensitivity of the procedure did not allow us to decide unequivocally between the second and third alternatives. In addition, we are presently unable to rule out the possibility that all three scenarios may occur in a single chain of cells. It is important to note that once FtsZ moves from incompletely constricted sites to begin septation elsewhere, the protein does not return to the original, partially constricted sites (1). This behavior may explain why most septa in the amidase mutants are never completed. Overall, the evidence supports the idea that murein hydrolases affect the behavior of FtsZ and that FtsZ vacates stalled septa.

At present, though, we cannot say whether it is the absence of FtsZ that stalls septal growth in the first place or whether the failure of septa to invaginate triggers the eviction of FtsZ.

Septum orientation. The long-standing question of how a bacterium directs its division apparatus to the center of the cell has been solved in its general outline (6, 44, 54). With this information, though, a new question arises as to how the cell ensures that its septum has the proper geometry and orientation. In particular, how is it that the septum invaginates symmetrically and exactly perpendicular to the side walls? Although the MinC and SlmA inhibitory proteins restrict the formation of the FtsZ ring to the central area of the cell and thus act as a “coarse control” for localizing the division site, there is evidence of room for error within this permissive zone. Indeed, highly asymmetric septa form in a variety of situations where the MinC and SlmA systems are still functional.

In this work we report that deleting amidase genes with or without the removal of PBP5 creates unnatural septa with high frequency. This behavior is consistent with many observations linked to the activity of other PG hydrolases. For example, deleting PBP5 along with additional endopeptidases or amidases leads to abnormal septation (40), and the original *E. coli envC* mutant produced tilted, multiple, closely spaced and incomplete septa, “as if there were several unsuccessful attempts at division” (43). In an *envC minCDE* mutant, spiral and double rings of ZipA-GFP are common in chains of cells (5), although because MinC was absent, the permissive zone for septum formation may have been enlarged. Nevertheless, the results argue that even in the presence of MinCDE and SlmA, the cell retains a degree of freedom in the placement and orientation of septa, which implies that there must be a “fine control” mechanism that decreases errors of septal formation within this zone.

The PG hydrolases of gram-positive bacteria clearly affect the positioning and geometry of cell division. In *Staphylococcus aureus*, the Atl protein is processed to yield two hydrolases, an amidase and glucosaminidase (49), and strains lacking Atl grow as clusters of unseparated cells (50). Mutants lacking the Sle1 *N*-acetylmuramyl-L-alanine amidase have multiple, misplaced, and sometimes curved septa that are positioned at odd angles so that they do not bisect daughter cells equally, effects that are magnified greatly in an *atl sle1* double mutant (29). In *B. subtilis*, the absence of the LytE murein hydrolase produces curved or bent cells that have unnatural lengths and widths (9). Removal of the PcsB protein, which has the characteristics of a murein hydrolase active during cell separation (7, 39), causes similarly aberrant cell division in several streptococci. A *pcsB* mutant of *Streptococcus agalactiae* grows in clumps because division septa are placed at unnatural (tilted) angles that produce “kinked” chains of cells whose size and shape are not uniform (41, 42). An *S. pneumoniae pcsB* mutant grows in long chains with multiple misplaced, tilted, aberrant, and unordered septa that create dramatically kinked chains (36). *Streptococcus mutans* lacking its *pcsB* homologue (*sagA*) produces misshapen cells with aberrant and “wavy” septal ingrowth and placement (11), and *Streptococcus thermophilus* deleted of its homologue (*cse*) grows in extremely long chains (7).

The overall impression is that in both gram-negative and gram-positive organisms, the PG hydrolases are essential for creating septa having the proper geometry and orientation. But

how might cutting the PG affect the symmetrical organization of the septal ring? Most of the divisome components are cytoplasmic or embedded in the cytoplasmic membrane, so there must be a connection between PG hydrolysis and the ability of cytoplasmic regulators to create a geometrically correct septum. One excellent possibility is that the hydrolases affect continuing PG synthesis (discussed above), which then affects septal morphology in a manner not yet determined. Indirect evidence that this relationship is important comes from interrupting PG synthesis by sequestering lipid II with the antibiotic nisin (27). In *B. subtilis*, cells treated with sublethal concentrations of nisin often produce multiple closely spaced septa, some of which are tilted (27), implying that the rate of PG synthesis affects not just the formation of septa but also their ultimate geometry.

A final possibility is that the outer membrane or something embedded within it is critical for creating appropriate septal morphology. This alternative must be kept in mind because the outer membrane may be poorly connected to the septal region in hydrolase mutants. Other suggestive evidence for this alternative is that the removal of O antigen from the outer membrane of *E. coli* also increases cell shape abnormalities (19).

Septal characteristics. Compared with the lateral walls, the poles of *E. coli* are relatively inert to incorporation of new PG and outer membrane material (16, 17, 32). It is not known when the septum becomes inert or what changes make it so because no differences in PG composition have been found to account for the difference. Our data indicate that the septum becomes inert immediately as it is synthesized or very soon thereafter, which in turn implies that PG in the vicinity of an SP ring is inert. The darkly stained nature of SP rings in electron and fluorescence microscopy implies that PG at these positions has a different structure from that present in other parts of the sacculus (22). In fact, these heavily stained bands are more resistant to digestion by muramidase but more sensitive to digestion by AmiC or the endopeptidase MepA (22). Alternatively, the increased staining of SP rings may simply reflect the fact that the PG is more concentrated or more highly cross-linked at these positions. In any case, the rapidity with which the PG becomes inert strongly suggests that the responsible characteristic must be generated while invagination is progressing. Currently, the most easily envisioned changes would be those created by the actions of one or more hydrolases while splitting SP rings. For example, amidases may denude the PG of a population of peptide side chains so that the region can no longer act as a recipient for the insertion of new monomers. It may be possible to test this idea if mutants can be forced to use individual hydrolases to complete invagination and cell separation; we could then see whether certain hydrolases leave the PG susceptible to further incorporation.

Challenges in identifying the physiological activities of murein hydrolases. It seems clear that few (if any) of the known, independent PG hydrolases are required for inserting PG precursors into the existing wall during normal cell elongation. It also appears that many (or most) affect the numbers of cells in chains, at least when multiple hydrolase genes are deleted. Does this then mean that most hydrolases are involved in cell separation? We suggest that great care must be exercised in making this claim about any particular enzyme. Specifically, we caution against using the number of cells in indi-

vidual chains as the sole measure to infer that a protein participates directly in septal splitting leading to cell separation.

The numbers of cells in chains and the lengths of these chains depend on the rate of PG synthesis, the rate of septal splitting, and, importantly, the frequency with which cells die and lyse. Mutations in the hydrolases may affect any of these processes, though only one is strictly associated with cell separation. For example, it is possible that specific hydrolases might be required for SP synthesis as proposed in the original multienzyme complex hypothesis (26). If so, then chain length would increase because constriction would slow or abort. In this scenario, an increase in chain length would represent the disruption of a synthetic complex rather than a deficiency in cell separation per se. A second alternative is that one or more of the murein hydrolases may lyse cells more frequently when expressed in particular mutants. Most hydrolases are lethal and lytic when overexpressed, so it would not be surprising if some were to behave similarly when underlying enzymatic balances were disturbed. In such mutants, chain lengths would be shortened because internal cells would lyse (at random), causing longer chains to break apart at these positions. We find evidence to support this possibility in the observation that many cell chains possess dead cells at their ends. Also consistent with this interpretation is the appearance at the ends of chains of lysozyme-treated cultures of “barbell-shaped” structures that are composed of multiple spheroplasts connected by a continuous outer membrane (23). We suggest that such structures are created when lysozyme removes the easily accessible PG from dead cells at the ends of the chains.

So, how do the preceding considerations impact our understanding of the physiological roles of the murein hydrolases? For one thing, although we may be able to present a putative order in which the hydrolases may act, this does not of itself indicate the actual function being played by each of the enzymes. Perhaps EnvC is required for PG synthesis at the septum; perhaps AmiA lyses cells and reduces chain length in the absence of AmiC; AmiC may be a true septum-splitting enzyme; or other permutations of the above possibilities may be true. Considering a specific example, when the very lytic Slt70 transglycosylase is removed from cells that lack AmiABC, the percentage of total cells in chains does not change but the number of cells in each chain increases by about twofold (22). Is this because Slt70 helps split the septum, or might it be that in the absence of Slt70, septal synthesis stalls or fewer cells lyse so that the chains grow longer? At present, there is no way to distinguish between these alternatives by using the coarse assay of chain length. New methods need to be devised to investigate the specific physiological roles of each of the hydrolases. Nonetheless, a relatively firm overall conclusion is that most hydrolases seem to function during cell division instead of during elongation of the lateral wall.

ACKNOWLEDGMENTS

This work was supported by grant GM061019 from the National Institutes of Health (to K.Y.), by grant PR2005-0024 of the Programa de Estancias de Profesores de Universidad e Investigadores del C.S.I.C. en Centros de Enseñanza Superior e Investigación Extranjeros y Españoles from the Spanish Ministry for Education and Science (to M.A.P.), and by an NSF North Dakota-EPSCoR Dissertation grant (to R.P.).

REFERENCES

1. Addinall, S. G., C. Cao, and J. Lutkenhaus. 1997. Temperature shift experiments with an *ftsZ84*(Ts) strain reveal rapid dynamics of FtsZ localization and indicate that the Z ring is required throughout septation and cannot reoccupy division sites once constriction has initiated. *J. Bacteriol.* **179**:4277–4284.
2. Addinall, S. G., and J. Lutkenhaus. 1996. FtsZ-spirals and -arcs determine the shape of the invaginating septa in some mutants of *Escherichia coli*. *Mol. Microbiol.* **22**:231–237.
3. Ayala, J. A., T. Garrido, M. A. de Pedro, and M. Vicente. 1994. Molecular biology of bacterial septation, p. 73–101. In J.-M. Ghuyssen and R. Hakenbeck (ed.), *Bacterial cell wall*. Elsevier Science B.V., Amsterdam, The Netherlands.
4. Bernhardt, T. G., and P. A. de Boer. 2003. The *Escherichia coli* amidase AmiC is a periplasmic septal ring component exported via the twin-arginine transport pathway. *Mol. Microbiol.* **48**:1171–1182.
5. Bernhardt, T. G., and P. A. de Boer. 2004. Screening for synthetic lethal mutants in *Escherichia coli* and identification of EnvC (YibP) as a periplasmic septal ring factor with murein hydrolase activity. *Mol. Microbiol.* **52**:1255–1269.
6. Bernhardt, T. G., and P. A. de Boer. 2005. SlmA, a nucleoid-associated, FtsZ binding protein required for blocking septal ring assembly over chromosomes in *E. coli*. *Mol. Cell* **18**:555–564.
7. Borges, F., S. Layec, A. Thibessard, A. Fernandez, B. Gintz, P. Hols, B. Decaris, and N. Leblond-Bourget. 2005. *cse*, a chimeric and variable gene, encodes an extracellular protein involved in cellular segregation in *Streptococcus thermophilus*. *J. Bacteriol.* **187**:2737–2746.
8. Buddelmeijer, N., and J. Beckwith. 2002. Assembly of cell division proteins at the *E. coli* cell center. *Curr. Opin. Microbiol.* **5**:553–557.
9. Carballido-Lopez, R., A. Formstone, Y. Li, S. D. Ehrlich, P. Noirot, and J. Errington. 2006. Actin homolog MreBH governs cell morphogenesis by localization of the cell wall hydrolase LytE. *Dev. Cell* **11**:399–409.
10. Charles, M., M. Perez, J. H. Kobil, and M. B. Goldberg. 2001. Polar targeting of *Shigella* virulence factor IcsA in *Enterobacteriaceae* and *Vibrio*. *Proc. Natl. Acad. Sci. USA* **98**:9871–9876.
11. Chia, J. S., L. Y. Chang, C. T. Shun, Y. Y. Chang, Y. G. Tsay, and J. Y. Chen. 2001. A 60-kilodalton immunodominant glycoprotein is essential for cell wall integrity and the maintenance of cell shape in *Streptococcus mutans*. *Infect. Immun.* **69**:6987–6998.
12. Dajkovic, A., and J. Lutkenhaus. 2006. Z ring as executor of bacterial cell division. *J. Mol. Microbiol. Biotechnol.* **11**:140–151.
13. De Las Rivas, B., J. L. Garcia, R. Lopez, and P. Garcia. 2002. Purification and polar localization of pneumococcal LytB, a putative endo-beta-N-acetylglucosaminidase: the chain-dispersing murein hydrolase. *J. Bacteriol.* **184**:4988–5000.
14. Denome, S. A., P. K. Elf, T. A. Henderson, D. E. Nelson, and K. D. Young. 1999. *Escherichia coli* mutants lacking all possible combinations of eight penicillin binding proteins: viability, characteristics, and implications for peptidoglycan synthesis. *J. Bacteriol.* **181**:3981–3993.
15. de Pedro, M. A., C. G. Grunfelder, and H. Schwarz. 2004. Restricted mobility of cell surface proteins in the polar regions of *Escherichia coli*. *J. Bacteriol.* **186**:2594–2602.
16. de Pedro, M. A., J. C. Quintela, J.-V. Höltje, and H. Schwarz. 1997. Murein segregation in *Escherichia coli*. *J. Bacteriol.* **179**:2823–2834.
17. de Pedro, M. A., K. D. Young, J. V. Höltje, and H. Schwarz. 2003. Branching of *Escherichia coli* cells arises from multiple sites of inert peptidoglycan. *J. Bacteriol.* **185**:1147–1152.
18. Gerding, M. A., Y. Ogata, N. D. Pecora, H. Niki, and P. A. de Boer. 2007. The trans-envelope Tol-Pal complex is part of the cell division machinery and required for proper outer-membrane invagination during cell constriction in *E. coli*. *Mol. Microbiol.* **63**:1008–1025.
19. Ghosh, A. S., A. L. Melquist, and K. D. Young. 2006. Loss of O-antigen increases cell shape abnormalities in penicillin-binding protein mutants of *Escherichia coli*. *FEMS Microbiol. Lett.* **263**:252–257.
20. Ghosh, A. S., and K. D. Young. 2005. Helical disposition of proteins and lipopolysaccharide in the outer membrane of *Escherichia coli*. *J. Bacteriol.* **187**:1913–1922.
21. Goehring, N. W., and J. Beckwith. 2005. Diverse paths to midcell: assembly of the bacterial cell division machinery. *Curr. Biol.* **15**:R514–R526.
22. Heidrich, C., M. F. Templin, A. Ursinus, M. Merdanovic, J. Berger, H. Schwarz, M. A. de Pedro, and J. V. Höltje. 2001. Involvement of N-acetylmuramyl-L-alanine amidases in cell separation and antibiotic-induced autolysis of *Escherichia coli*. *Mol. Microbiol.* **41**:167–178.
23. Heidrich, C., A. Ursinus, J. Berger, H. Schwarz, and J. V. Höltje. 2002. Effects of multiple deletions of murein hydrolases on viability, septum cleavage, and sensitivity to large toxic molecules in *Escherichia coli*. *J. Bacteriol.* **184**:6093–6099.
24. Höltje, J.-V. 1998. Growth of the stress-bearing and shape-maintaining murein sacculus of *Escherichia coli*. *Microbiol. Mol. Biol. Rev.* **62**:181–203.
25. Höltje, J.-V. 1993. “Three for one”—a simple growth mechanism that guarantees a precise copy of the thin, rod-shaped murein sacculus of *Escherichia*

- coli*, p. 419–426. In M. A. de Pedro, J.-V. Høltje, and W. Löffelhardt (ed.), Bacterial growth and lysis. Plenum Press, New York, NY.
26. Høltje, J.-V. 1996. A hypothetical holoenzyme involved in the replication of the murein sacculus of *Escherichia coli*. *Microbiology* **142**:1911–1918.
 27. Hyde, A. J., J. Parisot, A. McNichol, and B. B. Bonev. 2006. Nisin-induced changes in *Bacillus* morphology suggest a paradigm of antibiotic action. *Proc. Natl. Acad. Sci. USA* **103**:19896–19901.
 28. Ichimura, T., M. Yamazoe, M. Maeda, C. Wada, and S. Hiraga. 2002. Proteolytic activity of YibP protein in *Escherichia coli*. *J. Bacteriol.* **184**:2595–2602.
 29. Kajimura, J., T. Fujiwara, S. Yamada, Y. Suzawa, T. Nishida, Y. Oyamada, I. Hayashi, J. Yamagishi, H. Komatsuzawa, and M. Sugai. 2005. Identification and molecular characterization of an *N*-acetylmuramyl-L-alanine amidase Sle1 involved in cell separation of *Staphylococcus aureus*. *Mol. Microbiol.* **58**:1087–1101.
 30. Karibian, D., G. Pellon, and J. Starka. 1981. Autolysis of a division mutant of *Escherichia coli*. *J. Gen. Microbiol.* **126**:55–61.
 31. Koch, A. L. 1990. Additional arguments for the key role of “smart” autolysins in the enlargement of the wall of gram-negative bacteria. *Res. Microbiol.* **141**:529–541.
 32. Koch, A. L., and C. L. Woldringh. 1994. The metabolic inertness of the pole wall of a gram-negative rod. *J. Theor. Biol.* **171**:415–425.
 33. Miller, J. H. 1992. A short course in bacterial genetics: a laboratory manual and handbook for *Escherichia coli* and related bacteria. Cold Spring Harbor Laboratory Press, Cold Spring Harbor, NY.
 34. Mukherjee, A., C. N. Cao, and J. Lutkenhaus. 1998. Inhibition of FtsZ polymerization by SulA, an inhibitor of septation in *Escherichia coli*. *Proc. Natl. Acad. Sci. USA* **95**:2885–2890.
 35. Nanninga, N. 1991. Cell division and peptidoglycan assembly in *Escherichia coli*. *Mol. Microbiol.* **5**:791–795.
 36. Ng, W. L., K. M. Kazmierczak, and M. E. Winkler. 2004. Defective cell wall synthesis in *Streptococcus pneumoniae* R6 depleted for the essential PcsB putative murein hydrolase or the VicR (YycF) response regulator. *Mol. Microbiol.* **53**:1161–1175.
 37. Nilsen, T., A. S. Ghosh, M. B. Goldberg, and K. D. Young. 2004. Branching sites and morphological abnormalities behave as ectopic poles in shape-defective *Escherichia coli*. *Mol. Microbiol.* **52**:1045–1054.
 38. Ohnishi, R., S. Ishikawa, and J. Sekiguchi. 1999. Peptidoglycan hydrolase LytF plays a role in cell separation with CwF during vegetative growth of *Bacillus subtilis*. *J. Bacteriol.* **181**:3178–3184.
 39. Pagliero, E., O. Dideberg, T. Vernet, and A. M. Di Guilmi. 2005. The PECACE domain: a new family of enzymes with potential peptidoglycan cleavage activity in gram-positive bacteria. *BMC Genomics* **6**:19.
 40. Priyadarshini, R., D. L. Popham, and K. D. Young. 2006. Daughter cell separation by penicillin-binding proteins and peptidoglycan amidases in *Escherichia coli*. *J. Bacteriol.* **188**:5345–5355.
 41. Reinscheid, D. J., K. Ehlert, G. S. Chhatwal, and B. J. Eikmanns. 2003. Functional analysis of a PcsB-deficient mutant of group B streptococcus. *FEMS Microbiol. Lett.* **221**:73–79.
 42. Reinscheid, D. J., B. Gottschalk, A. Schubert, B. J. Eikmanns, and G. S. Chhatwal. 2001. Identification and molecular analysis of PcsB, a protein required for cell wall separation of group B streptococcus. *J. Bacteriol.* **183**:1175–1183.
 43. Rodolakis, A., P. Thomas, and J. Starka. 1973. Morphological mutants of *Escherichia coli*. Isolation and ultrastructure of a chain-forming *envC* mutant. *J. Gen. Microbiol.* **75**:409–416.
 44. Rothfield, L., A. Taghbalout, and Y. L. Shih. 2005. Spatial control of bacterial division-site placement. *Nat. Rev. Microbiol.* **3**:959–968.
 45. Sambrook, J., E. F. Fritsch, and T. Maniatis. 1989. Molecular cloning: a laboratory manual, 2nd ed. Cold Spring Harbor Laboratory Press, Cold Spring Harbor, NY.
 46. Sanchez-Puelles, J. M., C. Ronda, J. L. Garcia, P. Garcia, R. Lopez, and E. Garcia. 1986. Searching for autolysin functions. Characterization of a pneumococcal mutant deleted in the *lytA* gene. *Eur. J. Biochem.* **158**:289–293.
 47. Shockman, G. D., and J.-V. Høltje. 1994. Microbial peptidoglycan (murein) hydrolases, p. 131–166. In J.-M. Ghuysen and R. Hakenbeck (ed.), Bacterial cell wall. Elsevier Science B.V., Amsterdam, The Netherlands.
 48. Steinhauer, J., R. Agha, T. Pham, A. W. Varga, and M. B. Goldberg. 1999. The unipolar *Shigella* surface protein IcsA is targeted directly to the bacterial old pole: IcsP cleavage of IcsA occurs over the entire bacterial surface. *Mol. Microbiol.* **32**:367–377.
 49. Sugai, M., H. Komatsuzawa, T. Akiyama, Y. M. Hong, T. Oshida, Y. Miyake, T. Yamaguchi, and H. Suginaka. 1995. Identification of endo-beta-*N*-acetylglucosaminidase and *N*-acetylmuramyl-L-alanine amidase as cluster-dispersing enzymes in *Staphylococcus aureus*. *J. Bacteriol.* **177**:1491–1496.
 50. Takahashi, J., H. Komatsuzawa, S. Yamada, T. Nishida, H. Labischinski, T. Fujiwara, M. Ohara, J. Yamagishi, and M. Sugai. 2002. Molecular characterization of an *atl* null mutant of *Staphylococcus aureus*. *Microbiol. Immunol.* **46**:601–612.
 51. Trusca, D., S. Scott, C. Thompson, and D. Bramhill. 1998. Bacterial SOS checkpoint protein SulA inhibits polymerization of purified FtsZ cell division protein. *J. Bacteriol.* **180**:3946–3953.
 52. Weiss, D. S., J. C. Chen, J. M. Ghigo, D. Boyd, and J. Beckwith. 1999. Localization of FtsI (PBP3) to the septal ring requires its membrane anchor, the Z ring, FtsA, FtsQ, and FtsL. *J. Bacteriol.* **181**:508–520.
 53. Wientjes, F. B., and N. Nanninga. 1989. Rate and topography of peptidoglycan synthesis during cell division in *Escherichia coli*: concept of a leading edge. *J. Bacteriol.* **171**:3412–3419.
 54. Wu, L. J., and J. Errington. 2004. Coordination of cell division and chromosome segregation by a nucleoid occlusion protein in *Bacillus subtilis*. *Cell* **117**:915–925.
 55. Yamamoto, H., S. Kurosawa, and J. Sekiguchi. 2003. Localization of the vegetative cell wall hydrolases LytC, LytE, and LytF on the *Bacillus subtilis* cell surface and stability of these enzymes to cell wall-bound or extracellular proteases. *J. Bacteriol.* **185**:6666–6677.